

# Response to Reviewer's Comments concerning wes-2020-107

Thales Fava  
Frederik Zahle

Mikaela Lokatt  
Ardeshir Hanifi

Niels Sørensen  
Dan Henningson

We would like to thank the reviewer for careful and thorough reading of this paper. Our response follows.

## Referee #3 Comments

---

### Comments:

- **Comment:** L38-40: It is written that the PSE model are computational costly so not well suited for design. Nonetheless, the proposed model is based on PSE approach?  
**Answer:** We are thankful for noticing this mistake. The sentence has been corrected in the third paragraph of the Introduction of the revised document to: “The DNS approach for transition prediction provides accurate results, but it implies a high computational cost. With the current available computational power, simulations at Reynolds numbers corresponding to those on real wind turbines are not possible. The PSE analysis has a much lower computational cost compared to DNS [5], but it provides more accurate transition predictions than the RANS approach with an algebraic-integral or transport model.”
- **Comment:** L50: It is mentioned that the reference RANS solver (EllipSys3D) integrate a transition prediction tool based on database method. Which one? Are there any references available? In the previous sentence, Sorensen 2009 is given as a reference but this paper deals with gamma-Retheta method which is not a database method. Additionally, since RANS results will be used as comparison for transition prediction, does the database integrates 3D effect and/or rotational effects?  
**Answer:** The referee’s comment made us realize that the reference Sorensen (2009) was not the correct one to refer to the transition model used in the EllipSys3D solver for the current computations. The correct transition model is the semiempirical  $e^N$  method of Drela and Giles [2, 5]. This transition model does not integrate 3D nor rotational effects. This has been changed in the fifth paragraph of the Introduction of the revised document to: “Transition prediction within this solver is obtained through the semiempirical  $e^N$  method of Drela and Giles [2, 5]. This transition model does not account for effects of the blade rotation or the three-dimensional flow.”
- **Comment:** L73: The equations (for the mean flow as well as for the fluctuations) are given in the general case of compressible flow including the equation for the temperature (or the energy). Is there any interest in considering the general compressible case or could it be restricted to simplified incompressible formulation? For an angular velocity of  $\omega=1$  rad/s and a radius of  $r=100$ m the azimuthal velocity at the tip will be around 100m/s ie a Mach number of 0.3 which is the usual limit to separate incompressible to compressible regimes. Additionally, the RANS code is incompressible (mentioned Section 4, p10).  
**Answer:** We have implemented our model in the bl3D and NOLOT codes, which are validated and general-purpose boundary-layer and PSE codes, respectively. These codes use a compressible formulation. We agree with the reviewer that compressibility does not play a significant role in the current cases. However, since both codes run fast and do not present issues in the incompressible limit, we thought it was unnecessary to change their formulations to an incompressible

one. Thus, the compressible equations presented in the paper reflect the original equations implemented in the bl3D and NOLOT codes.

- **Comment:** L82: cp and gamma have already been used before. cp at the end of the abstract to refer to pressure coefficient and gamma in the gamma-Retheta model (ie referring to the intermittency function). It will be used again at the bottom of page 10 to refer to the intermittency factor. Additionally, page 9, equation 29 gamma is used as the angular frequency of the disturbances. A list of symbols at the beginning of the article will be helpful.

**Answer:** The referee's comment made us realize that the pressure coefficient should be " $C_p$ " and not " $c_p$ ", which is the specific heat at constant pressure. In the revised article,  $\gamma$  has been used only to refer to the intermittency factor, whereas  $\omega$  has been used to refer to the angular frequency of the disturbances and  $\Omega$  to the angular speed of the wind turbine. We agree with the reviewer that a list of symbols at the beginning would be helpful for the readers. There was such a list in a previous version of the document. However, including a list of symbols does not seem to be a common practice in WES. For this reason, we opted for removing it to comply with what seemed to be the editorial standard.

- **Comment:** L123: It is mentioned that the pressure can be obtained from the velocity and temperature variables. For me one quantity is missing: the density or the total pressure.

**Answer:** We agree with the referee that one needs the density or the total pressure to obtain the static pressure. In the second paragraph of Section 2.1.3 of the revised article, we have added the information that we used a reference density and the temperature obtained with the BL code to compute the pressure: "The density is calculated from the temperature and pressure using the equation of state and the BL approximation of pressure being constant inside the boundary layer. "

- **Comment:** L179-180: The PSE is derived from the continuity, **Navier-Stokes momentum** (better suited), energy and state equations.

**Answer:** We have changed from "Navier-Stokes" to momentum in the first paragraph of Section 3 of the revised document.

- **Comment:** L198 (Eq 27): Even though periodicity is assumed in x2 direction, 'q' and 'qtilde' depends on x2. Same remark for eq 28.

**Answer:** The variables 'q' and ' $\tilde{q}$ ' in equations 27 and 28 do not depend on  $x_2$ . They only depend on  $x_1$  and  $x_3$ .

- **Comment:** L205: Already mentioned but the angular frequency is quoted as gamma which has already been used as the intermittency.

**Answer:** We have removed this ambiguity.  $\gamma$  has been used only to refer to the intermittency factor, whereas  $\omega$  has been employed to denote the angular frequency of the perturbations.

- **Comment:** L217 (Eq33): the density fluctuation should also tend to 0 (or better be bounded) far away from the wall ( $x_3 \rightarrow \infty$ )

**Answer:** The reviewer is correct. However, since the PSE equations are differential equations of eight order, only eight boundary conditions are requested. Usually, these eight boundary conditions are imposed on the velocity and temperature perturbations. However, the far-field boundary condition for the wall-normal velocity component can be replaced with the one for the density. We have mentioned this in the fourth paragraph of Section 3 of the revised manuscript.

- **Comment:** L221: The definition of the N factor should be given here. How is it related to the amplitude function of the disturbances? Moreover it is often specified that it is an envelope N factor but never said that the envelope is a local maximum on frequency (I guess).

**Answer:** We are thankful for the remarks. We have included this definition at the end of Section 3 of the revised manuscript:

“ In the so-called  $e^N$  method, transition location is predicted based on the amplification of disturbances presented by the  $N$ -factors computed as

$$N = \ln(A/A_0) = \int_{x_0}^{x_1} \sigma(x) dx, \quad (1)$$

where  $A$  is the amplitude of the perturbations ( $A_0 = A(x_0)$ ),  $x_0$  the location where the perturbation first start to grow and  $\sigma$  the growth rate of the perturbation kinetic energy  $E$  defined as [3]

$$\sigma = \frac{1}{h_1} \left[ -\text{Im}(\alpha) + \text{Re} \left( \frac{1}{E} \frac{\partial E}{\partial x_1} \right) \right], \quad (2)$$

$$E = \int_0^\infty \bar{\rho} (\hat{u}_1^2 + \hat{u}_2^2 + \hat{u}_3^2) dx_3. \quad (3)$$

In the present work, we use the so-called *envelope-of-envelopes* method [1]. This means that transition is predicted by the envelope of  $N$ -factors, with all curves being computed for different pairs of  $\omega$  and  $\beta$ . This information has also been included at the end of Section 3.

- **Comment:** L255: It is mentioned that cp distributions are approximation/differ from RANS ones. It would be interesting to illustrate (quantify) this discrepancy on a figure all the more than in the following this argument is reiterated to justify the differences between BLX and RANS velocity profiles L307 as well as on transition locations L353 and L357.

**Answer:** We are thankful for the suggestion. We have added a section in the revised document (Section 4.2) to include Fig. 1 and discuss the differences between RANS and XFOIL pressure distributions.

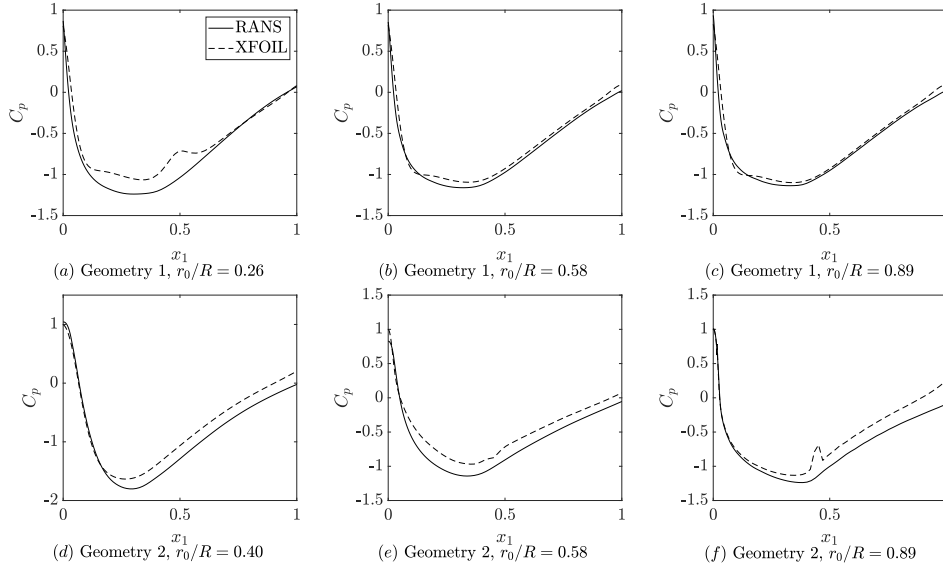


Figure 1: Comparison between XFOIL and RANS pressure distributions for the suction side of the airfoils of Geometries 1 and 2 at three radial positions.

- **Comment:** L284: “Although exhibiting higher values, the BLR and BLX profiles of spanwise velocity present the same shape of those from RANS.” I do not understand this sentence since in Fig 6b, RANS provide a  $u_2$  profile lower than zero (except close to the wall) while the  $u_2$  profile provided by BLR and BLX is positive.

**Answer:** We agree with the reviewer that this sentence is not correct. We have corrected it in the second paragraph of Section 4.4 of the revised document to: “Although the BLR and BLX profiles of spanwise velocity are close to each other, they indicate a positive velocity (flow towards the tip of the blade) whereas the spanwise velocity profile from RANS is only positive in the near-wall region.”

- **Comment:** L294: “This is similar to what was observed in Geometry 1 and may indicate the three-dimensional character of the flow at lower radii”. Not agree, related to the previous remark.  
**Answer:** We have changed the sentence in the fifth paragraph of the revised document to improve its accuracy: “This also occurs in a smaller extent at the inner radial position of Geometry 1 (Figs. 6a and 6b) where, at the near-wall region, the spanwise velocity profile presents an inversion of direction. The fact that the inversion of the spanwise velocity profile only occurs at the inner radial position of Geometries 1 and 2 may confirm the three-dimensional character of the flow at lower radii.”
- **Comment:** L337: The threshold value for eN method has been set up to 9 which is a typical value considering flight tests and quiet wind tunnel tests. Is this value appropriated for wind turbine blade application in the ‘atmospheric boundary layer’?  
**Answer:** We agree with the reviewer that  $N = 9$  represents transition in an environment with very low turbulence intensity (0.07 % according to Mack’s relation [4]), not representative of all atmospheric conditions. This value was selected in order to have a larger region of laminar flow in the RANS results, allowing a more detailed comparison between the results from the developed model and RANS, both in terms of the boundary-layer profiles and the transition location. The following sentence has been added to the first paragraph of Section 4.5 of the revised manuscript: “Although not representative of all atmospheric conditions, it is assumed  $N_{crit} = 9$  in the current work to have a larger region of laminar flow in the RANS results, allowing a more detailed comparison between the developed model and RANS.”
- **Comment:** L348: The PSE RANS results (not shown). It is unfortunate, since these results are the one to be considered as the reference to validate your approach. Is it possible to perform laminar RANS computations switching off the database transition prediction? Or rising the value of the transition threshold to obtain a laminar extend as long as possible in the RANS computation in order to analyze its stability with PSE? If not at least compare the evolution of the N factor between RANS and BLX for the first per cent of chord.  
**Answer:** We used a value of critical  $N$ -factor corresponding to natural transition ( $N = 9$ ) to force a larger laminar region in the RANS computations. The PSE analysis of the RANS base-flow revealed some modes amplified to a value lower than the critical  $N$ -factor. However, in most cases, spurious modes with large growth rates were obtained. The latter is probably related to numerical errors in the base-flow derivatives that had to be computed in the post-processing step. There were oscillations in some high-order derivatives that may stem from the precision of the base-flow variables as output by the EllipSys3D RANS solver and/or spatial oscillations in the flow field. Thus we have opted for removing references to the PSE RANS approach since we believe that there are not enough converged modes in this PSE analysis to generate a reliable envelope of  $N$ -factors.
- **Comment:** L384: “However, the modes tend to have a single-peaked structure at  $r_0/R = 0.26$ , associated with their high propagation angle (in absolute value).” This has to be related to the spanwise mean velocity profile (fig 6a and b) which is inflectional (ie sensitive to CF like disturbances)  
**Answer:** We agree with the reviewer that the single peak in the eigenfunction at  $r_0/R = 0.26$  is related to the inflectional spanwise velocity profile, which indicates sensitivity to crossflow-related disturbances. We have added the following explanation in the sixth paragraph of Section 4.5 of the revised manuscript: “The modes tend to have a single peak at this location, associated with their high  $|\Psi|$  and the inflectional spanwise velocity (Fig. 6b). This indicates that transition may be triggered by oblique TS or crossflow modes.”
- **Comment:** L434: “The single-peaked modes observed at  $r_0/R = 0.26$  for Geometry 1 and  $r_0/R = 0.40$  for Geometry 2 ( $\omega = 0.45$  rad.s-1) might represent an intermediate stage between a TS and crossflow transition”. Is there a shift/reduction of the frequency of the instability responsible for transition onset (the one reaching the Ncrit).  
**Answer:** The reduced frequency  $F$  of the perturbations leading to the transition onset in Geometries 1 and 2 are presented in Table 1.  $F$  decreases with the rotation speed (not monotonically

in Geometry 1 at  $r_0/R = 0.26$  and Geometry 2 at  $r_0/R = 0.89$ ). For low  $\Omega$ ,  $F$  is smaller at the inner radial position ( $r_0/R = 0.26$  and  $r_0/R = 0.40$ ). The increase in  $\Omega$  makes  $F$  at these locations become larger than at higher radii.

Geometry 1			
	$r_0/R = 0.26$	$r_0/R = 0.58$	$r_0/R = 0.89$
$\Omega = 0.32 \text{ rad.s}^{-1}$	F=1.86956E-05	F=1.98738E-05	F=2.19379E-05
$\Omega = 0.64 \text{ rad.s}^{-1}$	F=1.98087E-05	F=1.60444E-05	F=1.60297E-05
$\Omega = 0.96 \text{ rad.s}^{-1}$	F=1.54694E-05	F=1.32022E-05	F=1.43235E-05
Geometry 2			
	$r_0/R = 0.40$	$r_0/R = 0.58$	$r_0/R = 0.89$
$\Omega = 0.45 \text{ rad.s}^{-1}$	F=1.77893E-05	F=1.88131E-05	F=2.68559E-05
$\Omega = 0.90 \text{ rad.s}^{-1}$	F=1.64016E-05	F=1.29000E-05	F=1.15029E-05
$\Omega = 1.35 \text{ rad.s}^{-1}$	F=1.25585E-05	F=7.95290E-06	F=1.21288E-05

Table 1: Reduced frequency of the perturbations leading to the transition onset.

## References

- [1] D. Arnal and G. Casalis. “Laminar-turbulent transition prediction in three-dimensional flows”. In: *PROG AEROSP SCI* 36 (2000), pp. 173–191. DOI: 10.1016/S0376-0421(00)00002-6.
- [2] M. Drela and M. B. Giles. “Viscous-Inviscid Analysis of Transonic and Low Reynolds Number Airfoils”. In: *AIAA Journal* 25.10 (1987), pp. 1347–1355. DOI: 10.2514/3.9789.
- [3] A. Hanifi et al. *Linear nonlocal Instability Analysis - the linear NOLOT code*. Technical report FFA-TN 1994-54. Bromma, Sweden: The Aeronautical Research Institute of Sweden, 1994.
- [4] L. M. Mack. *Transition prediction and linear stability theory*. Technical report AGARD-CP-224. AGARD, 1977.
- [5] Ö. S. Özçakmak et al. “Laminar-turbulent transition characteristics of a 3-D wind turbine rotor blade based on experiments and computations”. In: *Wind Energy Science* 5.4 (2020), pp. 1487–1505. DOI: 10.5194/wes-5-1487-2020. URL: <https://wes.copernicus.org/articles/5/1487/2020/>.